Interfacial Passivation Engineering for Highly Efficient Quantum Dot Light-Emitting Diodes via Aromatic Amine-Functionalized Dipole Molecules

Fensha Cai,[†] Meng Li,*[, †] Han Zhang,[†] Yunqi Wang,[†] Zhe Li,[§] Yufei Tu,[‖] Mahmoud H. Aldamasy,[#] Xiaohong Jiang,[†] Bo Hou,[⊥] Shujie Wang,*[, †] Zuliang Du*[, †]

[†] Key Lab for Special Functional Materials of Ministry of Education, National & Local Joint Engineering Research Center for High-efficiency Display and Lighting Technology, School of Materials Science and Engineering, and Collaborative Innovation Center of Nano Functional Materials and Applications,
Henan University,
Kaifeng 475004, China

[§] School of Engineering and Materials Science (SEMS), Queen Mary University of London, London, E1 4NS UK

[‖] School of Electronics Information and Intelligent Manufacturing, Sias University, Xinzheng, China

[#] Helmholtz-Zentrum Berlin für Materialien und Energie GmbH. Hahn-Meitner-Platz 1, 14109 Berlin, Germany

[⊥] School of Physics and Astronomy, Cardiff University, Cardiff, Wales, CF24 3AA, UK

Keywords: quantum dot light-emitting diodes, dipole layer, interfacial defect, non-radiative recombination, operational stability

ABSTRACT: Blue quantum dot (QD) light-emitting diodes (QLEDs) exhibit unsatisfactory operational stability and electroluminescence (EL) properties due to severe non-radiative recombination induced by large numbers of dangling bond defects and charge imbalance in QD. Herein, dipolar aromatic amine-functionalized molecules with different molecular polarities are employed to regulate charge transport and passivate interfacial defects between QD and the electron transfer layer (ETL). The results show that the stronger the molecular polarity, especially with the $-CF_3$ groups possessing a strong electron-withdrawing capacity, the more effective the defects passivation of S and Zn dangling bonds at QD surface. Moreover, the dipole interlayer can effectively reduce electron injection into QD at high current density, enhancing charge balance and mitigating Joule heat. Finally, blue QLEDs with a peak external quantum efficiency (EQE) of 21.02% and a T_{50} operational lifetime exceeding 4000 hours at a luminance of 100 cd m^{-2}.

Quantum-dot light-emitting diodes promise great potential in display and lighting technologies due to their wider color gamut, chromatic purity, and solution-processability.[1-4] So far, the performance of the three primary colors (red, green, and blue) QLEDs has been rapidly developed due to optimizing QD materials, device structures, and fabrication processes.[5-8] State-of-the-art QLEDs have exhibited high EQE of over 20%, the T_{95} operating lifetimes of the three primary colors have reached 48000, 7500, and 227 h at an initial brightness of 1000 cd m^{-2}, respectively, and the red and green devices almost satisfy the requirements for low-brightness lighting and displays.[4, 9, 10] However, the operational stability and electroluminescence for blue QLEDs, especially at high brightness (high current density), are unsatisfactory.[9, 11]

Compared with red and green QLEDs, the wider bandgap of blue QD results in different interfacial charge transfer mechanisms. On the one hand, the vast hole injection barrier hinders hole injection, resulting in charge imbalance in the QD emitting layer[12-14,] especially at high current density. As a result, the Auger recombination rate increases, and efficiency roll-off (defined as the efficiency drops significantly at high current density).[15] On the other hand, the conduction band minimum (CBM) offset between the

QD and the ETL enables the excited electrons in blue QD to drift spontaneously. As a result, electrons accumulate at the ETL interface and deteriorate operational lifetimes.[16, 17] In addition, the higher surface area to volume ratio for blue QD than those of red and green QD results in many surface defects. These defects induce exciton quenching, signify surface-bulk coupling, and limit device efficiency and operational lifetime.[18-21] The key strategies implemented in blue QLEDs focus mainly on optimizing the functional layer materials and device structure.[22-27] However, these strategies did not consider the quality of QD itself and the interfacial electron transport concurrently. Designing molecules with functional groups that regulate interfacial charge transport and passivate defects at the same time is crucial. Molecules with thiophenol, primary amine, and halide ions have enormous potential to passivate QD surface states and regulate interfacial charge transport.[11, 22, 28, 29]

In this work, we used a series of aromatic amine-functionalized dipole molecules as interlayers in QD/ETL to passivate interfacial defects and reduce electron injection. The molecules that form the interfacial dipole layer are based on the commonly used PEAI. Through introducing fluorine atom to form 4-Fluorophenethylammonium iodide (F-PEAI) and -CF_3 group to form 4-(Trifluoromethyl) phenethylammonium iodide (CF_3-PEAI) at the *para* position of the amino group to regulate the electric dipole moment. Based on density functional theory (DFT) simulation and experimental characterizations, we demonstrated that the stronger the molecular polarity, especially with the inclusion of the -CF_3 groups possessing a strong electron-withdrawing capacity, the more efficient the interfacial defects passivation (S and Zn dangling bonds) at the QD surface. Moreover, the real-time temperature and the capacitance-voltage (*C-V*) characteristics of QLEDs revealed that the dipole layer could reduce electron injection at high current densities, thereby reducing Auger recombination and enhancing efficiency. As a result, our devices demonstrated an EQE of up to 21.02% with the turn-on voltage (voltage at a luminance of 1 cd m^{-2}) of about 2.4 V. Moreover, the T_{50} operation lifetime is enhanced by 6-fold from 631 h to 4051 h at an initial luminance of 100 cd m^{-2}.

A series of aromatic amine-functionalized dipole molecules, including PEAI, F-PEAI, and CF_3-PEAI have been employed as an interlayer in the QD/ETL interface optimization. **Figure 1a** displays molecular structures of oleic acid (OA), dipole molecules and the process of solid-state interfacial engineering. We show that the dipole layers would not affect UV-vis absorption, band gap (**Figure S1**), and morphology of pristine QD (referring to P-QD) films. Atomic force microscope (AFM) images confirm that all the layers were pinhole-free (**Figure S2**), the root mean squared roughness (RMS) of P-QDs was 1.23 nm, and it showed no noticeable change for dipole layers modified QD (referring to DL-QD), which suggested a uniform coverage of the surface of P-QDs with no agglomeration.

It is worth noting that the dipole layers could slightly increase the optical properties of the QD films. **Figure 1b** shows the steady-state photoluminescence (PL) spectra of P-QD and DL-QD films to investigate the influence of dipole layers on the fluorescence property of QD. The significantly increased PL intensity for DL-QD showed the efficacy of interfacial engineering in passivating defects effectively. The time-correlated single photon counting (TCSPC) measurements (**Figure 1c**) were performed, and the decay curves were fitted with bi-exponential models. It revealed that the PL lifetime increased to 5.04 (PEAI), 5.46 (F-PEAI), and 5.96 ns (CF_3-PEAI) for DL-QD compared with the P-QD films of 3.57 ns. The results are consistent with the PL measurements, proving the passivation of surface defects by the dipole layers, implying suppressed exciton quenching process.[11]

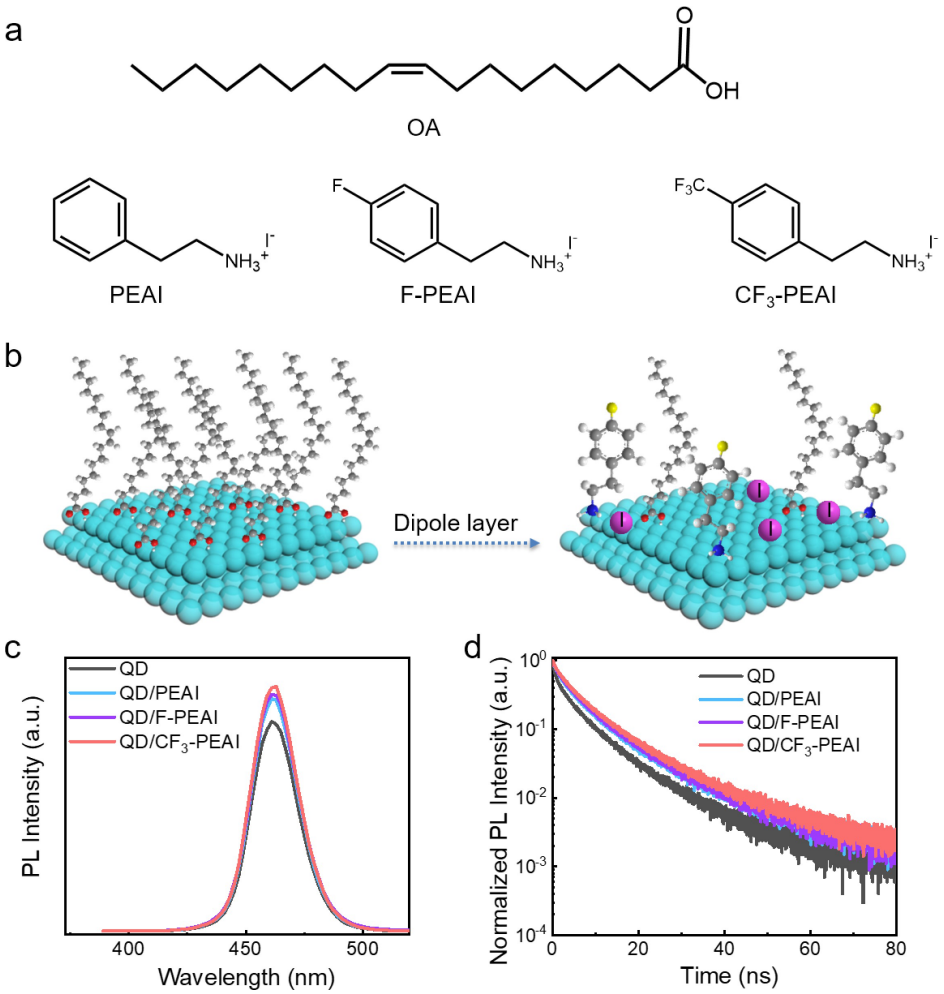

Figure 1. (a) The molecular structures of OA, PEAI, F-PEAI, and CF_3-PEAI. (b) Schematic illustration of the dipole layer treatment on QD films. (c) PL spectra and (d) TCSPC decay curves of the P-QD and DL-QD films.

The interaction between dipole layers and QD films was also investigated by X-ray photoelectron spectroscopy (XPS) measurements. The XPS spectra of N 1s and I 3d peaks shown in DL-QD films indicate the existence of the dipole layers on the surface of QD films (**Figure 2a** and **b**). The Zn 2p peaks of the PEAI, F-PEAI, and CF_3-PEAI-passivated QD film shift towards higher binding energy by 0.15 eV, 0.25 eV, and 0.3 eV (**Figure 2c**), respectively. We attribute these slight shifts to the dipole layers' stronger interaction with QD because of their strong affinity. To further clear this point, we performed Fourier transform infrared spectroscopy (FTIR), as shown in **Figure 2d**. The carbon-oxygen (COO^-) bond stretching frequency at 1,550 cm^{-1} and 1,454 cm^{-1}, C-H stretching vibrations signals of the methylene group (CH_2) at 2,931 cm^{-1} and 2,854

cm^{-1} in OA is significantly reduced, indicating that most OA ligands have been replaced with the dipolar molecules.[22, 30] This will increase the QD overall performance such as optical properties and stability as OA ligands readily shed from the surface of QDs, inducing dangling bonds, surface defect states, or even QD aggregation.

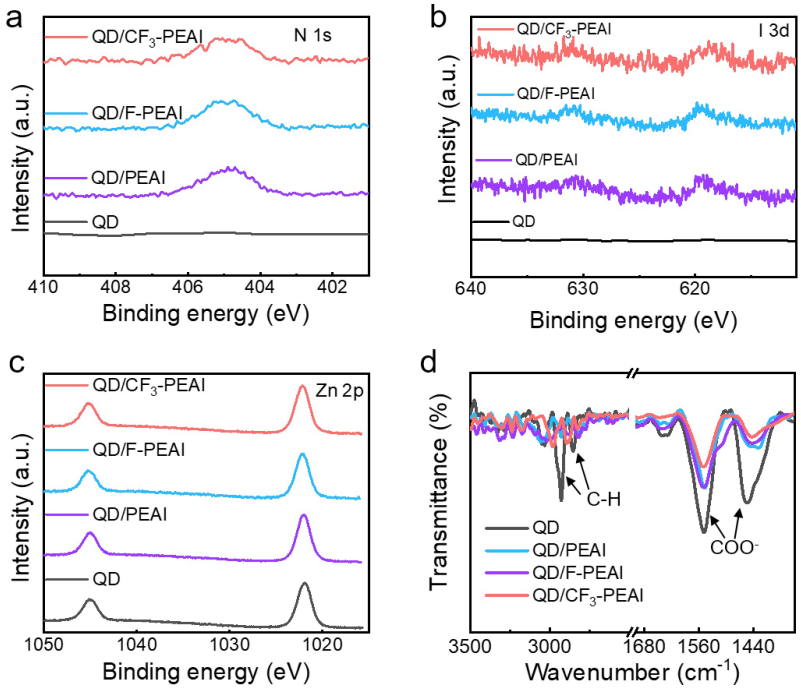

Figure 2. XPS spectra of (a) N 1s, (b) I 3d, and (c) Zn 2p core level peaks of P-QD and DL-QD films. (d) FTIR spectra of P-QD and DL-QD films.

To study the effect of dipole layers' molecular polarity on the defects of QD films, we calculated the electrostatic potential (φ) of PEAI, F-PEAI, and CF_3-PEAI using DFT simulations. As shown in **Figure 3a**, the electron-withdrawing group of -F and -CF_3 on the acceptor part presents a high electron density. The electron-deficient area exists mainly on the site of ammonium cations (-NH_3^+), providing favorable conditions for binding with the exposed dangling bond defects. The maximum electrostatic potential (φ_{max}) at the -NH_3^+ side for the three passivation dipole layer molecules are determined to be: $\varphi_{max,PEA} < \varphi_{max,F\text{-}PEA} < \varphi_{max,CF3\text{-}PEA}$. CF_3-PEAI has the most significant electrostatic potential, which means the highest dipole moment among the three molecules. We postulate that this molecular polarity difference could affect the surface adsorption of -NH_3^+ to negatively charged defects (such as S dangling bonds) on the

ZnS shell. We carried out DFT simulations to study the surface adsorption and defect passivation for the three dipole layer molecules (see details in the Experimental section in supporting). **Figure 3b and c** illustrate the adsorption energy (E_{ads}) and defect passivation between QD and dipole molecules. The previous reports showed that zinc vacancies (V_{Zn}) and sulfur vacancies (V_S) have lower defect formation energy than sulfur interstitials (S_{int}), and zinc interstitials (Zn_{int}), which are two dominant defects in ZnS, indicating S atoms and Zn atoms are exposed on the (111) ZnS surface.[31, 32] The X-ray diffraction (XRD) plots of QD in **Figure S3** confirmed the shell of QD is consistent with a zinc blende structure of ZnS.[1] **Figure S4** illustrates E_{ads} of QD and OA ligands. The E_{ads} of OA, PEAI, F-PEAI, and CF_3-PEAI passivated (111) ZnS surfaces are -0.661, -3.161, -3.165 and -3.275 eV, respectively. CF_3-PEAI binds to the QD most strongly due to its highest φ_{max} among the three dipole layer molecules. We found that the binding energy of dipolar layer molecules to QD is much higher than that of the OA ligand, which could enhance the stability of QD.[1,28] A stronger binding with the ZnS surface suggests a more effective surface passivation because defective sites are more likely to be passivated, according to the TCSPC result. Moreover, our calculation showed that iodide ions bound to Zn dangling bonds stabilized the surface energy. These results indicate that interfacial engineering has a great potential to reduce exciton quenching and improve radiative recombination.

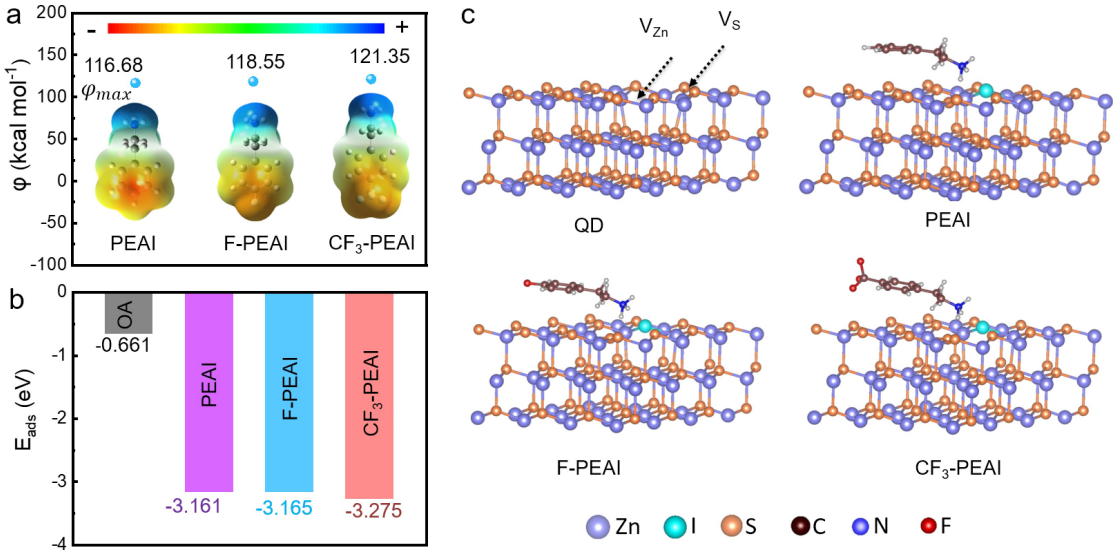

Figure 3. (a) Dipolar layer molecule's Electrostatic potential (φ). (b) Binding energy

between QD and OA ligand and dipole molecules. (c) Calculated E_{ads} and surface defect passivation of QD and dipole molecules.

To investigate the dipole molecule's passivation effect on the QLEDs performance, we fabricated QLEDs with the configuration ITO/PEDOT:PSS/PF8Cz/P-QD (DL-QD)/ETL/Al (**Figure 4a**). The luminescent layer CdSe/ZnSe/ZnS core/shell QD and the ETL of the ethylenediaminetetraacetic acid dipotassium salt (EDTAK) functionalized ZnO (EK-ZnO) in this work are the same as our previous report.[33] **Figure 4b** shows the device energy level diagram, and the energy band structures of PF8Cz, QD, and EK-ZnO were quoted from the reported literature.[4, 33] **Figuree S6** presents the EL spectra of QLEDs based on DL-QDs located at 468 nm, with no spectral trace from the adjacent charge transport layer, illustrating an efficient exciton radiative recombination only occurring at the QDs. Notably, the EL peaks exhibit no obvious red-shift with the increasing driving voltage from 2.4 to 6.0 V, indicating significant EL spectra stability. The EL peaks correspond to the Commission Internationale de L'Eclairage (CIE) color coordinates of (0.1312, 0.0752) (**Figure S7**). **Figure 4c** shows the current density-luminance-voltage (*J-V-L*) characteristics of QLEDs based on P-QD and DL-QD. The turn-on voltage is ~2.5 V for all QLEDs. Interestingly, the current density at high voltage was decreased evidently after interfacial engineering, i.e., the current density for control devices at 4 V was 853 mA/cm^2 and reduced to 471 mA/cm^2 for CF_3-PEAI-treatment-QD-based devices. However, the maximum luminance improved from 14360 cd m^{-2} to 20070 cd m^{-2}. We attributed these characteristics to the reduced defect states and the reduced electron injection after interfacial engineering, which effectively restrained non-radiative recombination.[34, 35] **Figure 4d** shows the EQE-luminance-current efficiency (*EQE-L-CE*) characteristics of these devices**.** Benefit from the defect passivation effect and the reduction of non-radiative recombination, the obtained EQE increased from 15.29% (control) to 16.80% (PEAI), 18.27% (F-PEAI) and finally to 21.02% (CF_3-PEAI). The corresponding current efficiency increased from 8.63 (control) to 10.54 (PEAI), 12.88 (F-PEAI), and finally to 13.80 cd A^{-1} (CF_3-PEAI). The relevant device parameters are summarized in **Table**

S1. Notoriously, the EQE peak values are commonly achieved at low current densities and usually exhibit a quick roll-off with increasing current density, especially for blue QLEDs.[6, 36, 37] Notably, our devices show higher EQE and lower efficiency roll-off. To clarify the efficiency roll-off quantitatively, we introduce a critical parameter, L_{80}, corresponding to the luminance at which the EQE drops to 80% of its maximum value. As shown in **Figure S5,** the L_{80} value is increased from 7819 cd/cm^2 to 12300 (PEAI), 13043 (F-PEAI), and finally to 13800 cd cm^{-2} (CF_3-PEAI), which means the efficiency roll-off has been effectively suppressed in dipole layer-based devices. **Figure 4e** shows the histogram of the maximum EQE of the devices before and after interfacial engineering. The average EQE of the 21 devices was 14.46% with a low standard deviation of 0.85 for the control device and 19.81% with a low standard deviation of 0.83 for the optimized device, suggesting high reproducibility. The measured T_{50} operational lifetime (the time taken for luminance to drop to 50% of its initial value) of the CF_3-PEAI-treated device was 6.5 h at a constant current density of 38.7 mA cm^{-2}, corresponding luminance of 5040 cd/m^2 (**Figure 4f**), equivalent to 4051 h at 100 cd/m^2 by applying an acceleration factor of 1.64.[38, 39] This device's lifetime is around 6-fold longer than the control devices, where the measured value was 2.8 h under a constant current density of 39.2 mA cm^{-2}, and the converted value was 631 h. The enhanced operational lifetime for the optimized devices is attributed to reduced interfacial defects and electron injection at high voltage, which significantly reduced non-radiative recombination.

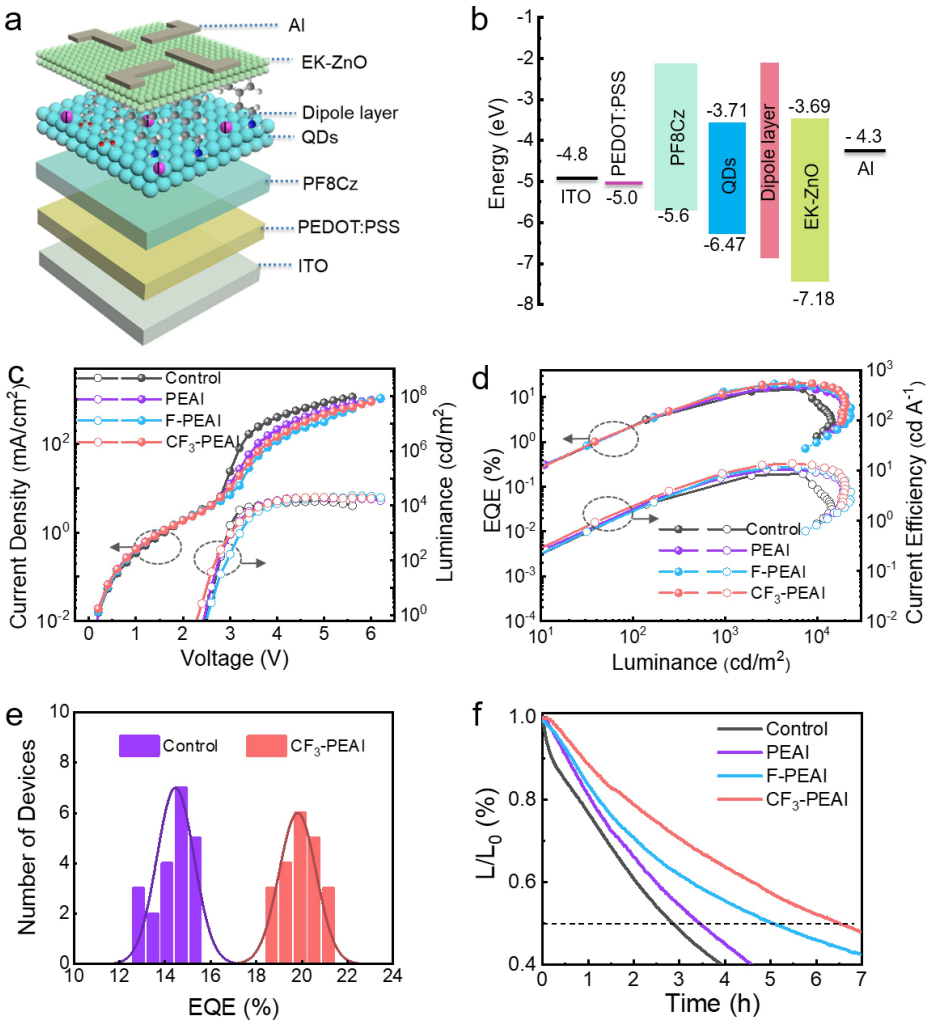

Figure 4. QLEDs performance based on P-QD and DL-QD films. (a) Device structure. (b) Device energy level diagram. (c) J-L-V characteristics. (d) EQE-L-CE characteristics. (e) Histograms of peak EQEs from 21 QLEDs. (f) Operational lifetime.

We measured the Joule heat generated during device operation to identify the reduced non-radiative recombination. **Figure 5a** shows the monitored real-time temperature of QLEDs before and after interfacial engineering using an infrared thermal camera. The surface temperature images of the working QLEDs were captured after applying a specific voltage for 3min. For the control QLEDs, the surface temperature is sharply increased from 26.4 °C at 0 V to 34.7 °C at 8 V. Compared with the control device, the Joule heat is effectively dissipated for the CF_3-PEAI-treated device, and the surface temperature is mildly increased from 26.4 °C at 0 V to 30.8 °C at 8 V. Heat generation rate, and value are significantly suppressed, especially at high voltage, according to the

J-V characteristic. It should be noted that the internal temperature of the working device should be higher than the measured surface temperature due to the low thermal conductivity of the functional layers in QLEDs.

To further demonstrate the reduction of electron injection after the interfacial engineering, the electron-only devices (EODs) and C-V characteristics were performed. The EOD structure is ITO/EK-ZnO/QD/EK-ZnO/Al (inset of **Figure 5b**). The current density is sharply suppressed by the CF_3-PEAI-treated device, indicating the suppression of electron injection (**Figure 5b**). In addition, **Figure 5c** shows the C-V characteristics under the frequency of 5 kHz. Around zero bias, the capacitances were determined by geometrical capacitance in both devices. The capacitances start to increase indicating that electrons were injected and accumulated in the device, because of the higher electron mobility and minimal barrier than hole. When the capacitances start to decrease, means holes injected and recombines with the accumulated electrons. It is clear that the device based on CF_3-PEAI-treated exhibits lower peak capacitances, meaning the reduced of electrons injection, thus reducing non-radiative recombination.[40, 41]

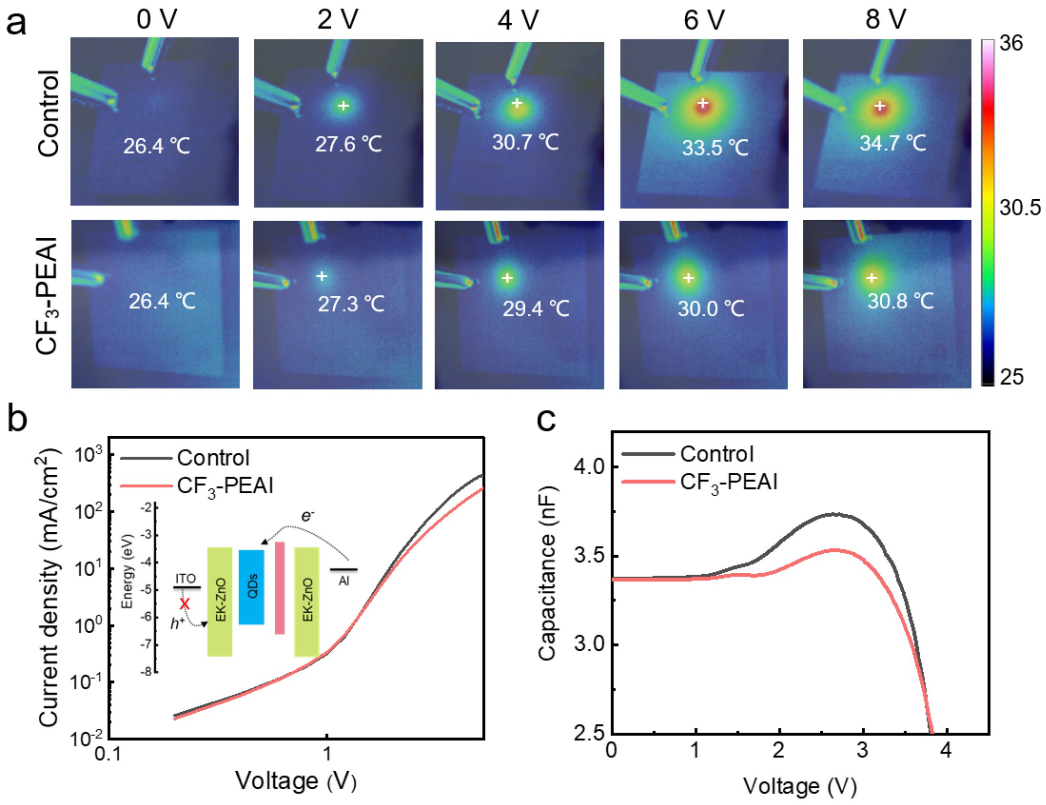

Figure 5. (a) Surface temperature images of QLEDs based on P-QD and CF_3-PEAI-treated QD at various voltages. (b) J-V characteristics of the EODs and (c) C-V characteristics of the device based on P-QD and CF_3-PEAI-treated QD.

In summary, we report the interfacial engineering strategy to achieve high efficiency, low-efficiency roll-off, and excellent operational stability in blue QLEDs. A series of aromatic amine-functionalized dipole molecules with different molecular polarities were introduced as interfacial layers to passivate QD surface dangling bond defect. We demonstrate that dipole molecule CF_3-PEAI with higher polarity exhibits better defect passivation due to the strong binding energy to the QD surface S dangling bond. In addition, the dipole layer could alleviate electron excess injection, especially at high current density, resulting in suppressed non-radiative recombination and efficiency roll-off. The resulting blue QLEDs demonstrate a high EQE of 21.02% and a maximum brightness of 20070 cd m^{-2}. More importantly, benefiting from suppressing defect states and Joule heat, our device has a long-operational lifetime of T_{50}@100 cd m^{-2} 4051 h. The interfacial strategy contributes a facile route towards efficient and stable blue QLEDs for next-generation displays.

ASSOCIATED CONTENT

Supporting Information

This material is available free of charge via the Internet at http://pubs.acs.org.

Supplementary information of the materials; fabrication of QLEDs; Theoretical calculations; Characterization methods, molecular structures of oleic acid and dipole molecules; UV-vis absorption spectra and AFM images of the P-QD and DL-QDs films; normalized EQE-L characteristics, EL spectra, and CIE of QLEDs based on CF_3-PEAI-treated-QD.

AUTHOR INFORMATION

Corresponding Authors

Meng Li — *Key Lab for Special Functional Materials of Ministry of Education, National & Local Joint Engineering Research Center for High-efficiency Display and Lighting Technology, School of Materials Science and Engineering, and Collaborative Innovation Center of Nano Functional Materials and Applications, Henan University, Kaifeng 475004, China*
E-mail: *mengli@henu.edu.cn*
Shujie Wang — *Key Lab for Special Functional Materials of Ministry of Education, National & Local Joint Engineering Research Center for High-efficiency Display and Lighting Technology, School of Materials Science and Engineering, and Collaborative Innovation Center of Nano Functional Materials and Applications, Henan University, Kaifeng 475004, China*
E-mail: *wsj@henu.edu.cn*
Zuliang Du — *Key Lab for Special Functional Materials of Ministry of Education, National & Local Joint Engineering Research Center for High-efficiency Display and Lighting Technology, School of Materials Science and Engineering, and Collaborative Innovation Center of Nano Functional Materials and Applications, Henan University, Kaifeng 475004, China*
E-mail: *zld@henu.edu.cn*

Authors
Fensha Cai — *Key Lab for Special Functional Materials of Ministry of Education, National & Local Joint Engineering Research Center for High-efficiency Display and Lighting Technology, School of Materials Science and Engineering, and Collaborative Innovation Center of Nano Functional Materials and Applications, Henan University, Kaifeng 475004, China ORCID:0009-0003-0555-2111*
Yamei Zhou — *Key Lab for Special Functional Materials of Ministry of Education, National & Local Joint Engineering Research Center for High-efficiency Display and Lighting Technology, School of Materials Science and Engineering, and Collaborative Innovation Center of Nano Functional Materials and Applications, Henan University, Kaifeng 475004, China*
Yufei Tu — *School of Electronics Information and Intelligent Manufacturing, Sias University, Xinzheng, China*
Mahmoud H. Aldamasy — *Helmholtz-Zentrum Berlin für Materialien und Energie GmbH. Hahn-Meitner-Platz 1, 14109 Berlin, Germany*

Xiaohong Jiang — *Key Lab for Special Functional Materials of Ministry of Education, National & Local Joint Engineering Research Center for High-efficiency Display and Lighting Technology, School of Materials Science and Engineering, and Collaborative Innovation Center of Nano Functional Materials and Applications, Henan University, Kaifeng 475004, China*

Bo Hou — *School of Physics and Astronomy, Cardiff University, Cardiff, Wales, CF24 3AA, UK ORCID: 0000-0001-9918-8223*

Author Contributions

M. L. supervision and conceived the concept of this work. F. C. carried out the experimental, analyzed the data, and wrote the original draft. H. Z., Y. W., and Y. T. provided instructions for the experiments. X. J. and B. H. contributed to optimization of the various experimental steps and supervision in this work. M.H. A. and Z. L. revised the manuscript. S. W. and Z. D. provided financial support and other necessary research resources. All authors reviewed the manuscript and discussed the results.

Notes

The authors declare no competing financial interest.

ACKNOWLEDGMENTS

We gratefully acknowledge the financial support from the National Natural Science Foundation of China (Grant No. 62234006, 62374052); National Key Research and Development Program of China (2022YFB3602901).

REFERENCE

1. Song, J.; Wang, O.; Shen, H.; Lin, Q.; Li, Z.; Wang, L.; Zhang, X.; Li, L. S., Over 30% External Quantum Efficiency Light-Emitting Diodes by Engineering Quantum Dot-Assisted Energy Level Match for Hole Transport Layer. *Adv. Funct. Mater.* **2019,** *29* (33), 1808377-1828385.
2. Li, B.; Lu, M.; Feng, J.; Zhang, J.; Smowton, P. M.; Sohn, J. I.; Park, I.-K.; Zhong, H.; Hou, B., Colloidal quantum dot hybrids: an emerging class of materials for ambient lighting. *J. Mater. Chem. C* **2020,** *8* (31), 10676-10695.
3. Osypiw, A. R. C.; Lee, S.; Jung, S.-M.; Leoni, S.; Smowton, P. M.; Hou, B.; Kim, J. M.; Amaratunga, G. A. J., Solution-processed colloidal quantum dots for light

emission. *Mater. Adv.* **2022,** *3* (17), 6773-6790.

4. Deng, Y.; Peng, F.; Lu, Y.; Zhu, X.; Jin, W.; Qiu, J.; Dong, J.; Hao, Y.; Di, D.; Gao, Y.; Sun, T.; Zhang, M.; Liu, F.; Wang, L.; Ying, L.; Huang, F.; Jin, Y., Solution-processed green and blue quantum-dot light-emitting diodes with eliminated charge leakage. *Nat. Photonics* **2022,** *16* (7), 505-511.
5. Moon, H.; Chae, H., Efficiency Enhancement of All-Solution-Processed Inverted-Structure Green Quantum Dot Light-Emitting Diodes Via Partial Ligand Exchange with Thiophenol Derivatives Having Negative Dipole Moment. *Adv. Opt. Mater.* **2019,** *8* (1), 1901314-1901318.
6. Wang, F.; Zhang, H.; Lin, Q.; Song, J.; Shen, H.; Zhang, H.; Ji, W., Suppressed efficiency roll-off in blue light-emitting diodes by balancing the spatial charge distribution. *J. Mater. Chem. C* **2020,** *8* (37), 12927-12934.
7. Cao, W.; Xiang, C.; Yang, Y.; Chen, Q.; Chen, L.; Yan, X.; Qian, L., Highly stable QLEDs with improved hole injection via quantum dot structure tailoring. *Nat. Commun.* **2018,** *9* (1), 2608-2613.
8. Yang, Y.; Zheng, Y.; Cao, W.; Titov, A.; Hyvonen, J.; Manders, J. R.; Xue, J.; Holloway, P. H.; Qian, L., High-efficiency light-emitting devices based on quantum dots with tailored nanostructures. *Nat. Photonics* **2015,** *9* (4), 259-266.
9. Chen, X.; Lin, X.; Zhou, L.; Sun, X.; Li, R.; Chen, M.; Yang, Y.; Hou, W.; Wu, L.; Cao, W.; Zhang, X.; Yan, X.; Chen, S., Blue light-emitting diodes based on colloidal quantum dots with reduced surface-bulk coupling. *Nat. Commun.* **2023,** *14* (1), 284-292.
10. Gao, Y.; Li, B.; Liu, X.; Shen, H.; Song, Y.; Song, J.; Yan, Z.; Yan, X.; Chong, Y.; Yao, R.; Wang, S.; Li, L. S.; Fan, F.; Du, Z., Minimizing heat generation in quantum dot light-emitting diodes by increasing quasi-Fermi-level splitting. *Nat. Nanotechnol.* **2023,** *18*, 1168-1174.
11. Kim, T.; Kim, K. H.; Kim, S.; Choi, S. M.; Jang, H.; Seo, H. K.; Lee, H.; Chung, D. Y.; Jang, E., Efficient and stable blue quantum dot light-emitting diode. *Nature* **2020,** *586* (7829), 385-389.
12. Cho, Y.; Lim, J.; Li, M.; Pak, S.; Wang, Z. K.; Yang, Y. G.; Abate, A.; Li, Z.; Snaith, H. J.; Hou, B.; Cha, S., Balanced Charge Carrier Transport Mediated by Quantum Dot Film Post-organization for Light-Emitting Diode Applications. *ACS Appl. Mater. Interfaces* **2021,** *13* (22), 26170-26179.
13. Liang, S.; Wang, S.; Wu, Z.; Wen, B.; Cai, G.; Jiang, X.; Huang, G.; Li, C.; Zhao,

Y.; Du, Z., Interfacial Charge Modulation: An Efficient Strategy for Stable Blue Quantum-Dot Light-Emitting Diodes. *Adv. Opt. Mater.* **2022,** *11* (2), 2201802-2201810.

14. Tian, D.; Ma, H.; Huang, G.; Gao, M.; Cai, F.; Fang, Y.; Li, C.; Jiang, X.; Wang, A.; Wang, S.; Du, Z., A Review on Quantum Dot Light-Emitting Diodes: From Materials to Applications. *Adv. Opt. Mater.* **2022,** *11*, 2201965-2201982.
15. Shirasaki, Y.; Supran, G. J.; Tisdale, W. A.; Bulović, V., Origin of Efficiency Roll-Off in Colloidal Quantum-Dot Light-Emitting Diodes. *Phys. Rev. Lett.* **2013,** *110* (21), 217403-217414.
16. Chang, J. H.; Park, P.; Jung, H.; Jeong, B. G.; Hahm, D.; Nagamine, G.; Ko, J.; Cho, J.; Padilha, L. A.; Lee, D. C.; Lee, C.; Char, K.; Bae, W. K., Unraveling the Origin of Operational Instability of Quantum Dot Based Light-Emitting Diodes. *ACS Nano* **2018,** *12* (10), 10231-10239.
17. Chen, S.; Cao, W.; Liu, T.; Tsang, S. W.; Yang, Y.; Yan, X.; Qian, L., On the degradation mechanisms of quantum-dot light-emitting diodes. *Nat. Commun.* **2019,** *10* (1), 765-773.
18. Cho, I.; Jung, H.; Jeong, B. G.; Chang, J. H.; Kim, Y.; Char, K.; Lee, D. C.; Lee, C.; Cho, J.; Bae, W. K., Multifunctional Dendrimer Ligands for High-Efficiency, Solution-Processed Quantum Dot Light-Emitting Diodes. *ACS Nano* **2017,** *11* (1), 684-692.
19. Rhee, S.; Hahm, D.; Seok, H. J.; Chang, J. H.; Jung, D.; Park, M.; Hwang, E.; Lee, D. C.; Park, Y. S.; Kim, H. K.; Bae, W. K., Steering Interface Dipoles for Bright and Efficient All-Inorganic Quantum Dot Based Light-Emitting Diodes. *ACS Nano* **2021,** *15* (12), 20332-20340.
20. Liu, X.; Wang, L.; Gao, Y.; Zeng, Y.; Liu, F.; Shen, H.; Manna, L.; Li, H., Ultrastable and High-Efficiency Deep Red QLEDs through Giant Continuously Graded Colloidal Quantum Dots with Shell Engineering. *Nano Lett.* **2023,** *23*(14), 6689-6697.
21. Xiang, C.; Wu, L.; Lu, Z.; Li, M.; Wen, Y.; Yang, Y.; Liu, W.; Zhang, T.; Cao, W.; Tsang, S.-W.; Shan, B.; Yan, X.; Qian, L., High efficiency and stability of ink-jet printed quantum dot light emitting diodes. *Nat. Commun.* **2020,** *11* (1), 1646-1654.
22. Cho, I.; Jung, H.; Jeong, B. G.; Hahm, D.; Chang, J. H.; Lee, T.; Char, K.; Lee, D. C.; Lim, J.; Lee, C.; Cho, J.; Bae, W. K., Ligand-Asymmetric Janus Quantum Dots for Efficient Blue-Quantum Dot Light-Emitting Diodes. *ACS Appl. Mater.*

Interfaces **2018,** *10* (26), 22453-22459.

23. An, H. J.; Baek, S. D.; Kim, D. H.; Myoung, J. M., Energy and Charge Dual Transfer Engineering for High-Performance Green Perovskite Light-Emitting Diodes. *Adv. Funct. Mater.* **2022,** *32* (21), 2112849-2112858.
24. Zhang, Z.; Ye, Y.; Pu, C.; Deng, Y.; Dai, X.; Chen, X.; Chen, D.; Zheng, X.; Gao, Y.; Fang, W.; Peng, X.; Jin, Y., High-Performance, Solution-Processed, and Insulating-Layer-Free Light-Emitting Diodes Based on Colloidal Quantum Dots. *Adv. Mater.* **2018,** *30* (28), 1801387-1801394.
25. Wang, F.; Hua, Q.; Lin, Q.; Zhang, F.; Chen, F.; Zhang, H.; Zhu, X.; Xue, X.; Xu, X.; Shen, H.; Zhang, H.; Ji, W., High-Performance Blue Quantum-Dot Light-Emitting Diodes by Alleviating Electron Trapping. *Adv. Opt. Mater.* **2022,** *10* (13), 2200319-2200326.
26. Gao, M.; Yang, H.; Shen, H.; Zeng, Z.; Fan, F.; Tang, B.; Min, J.; Zhang, Y.; Hua, Q.; Li, L. S.; Ji, B.; Du, Z., Bulk-like ZnSe Quantum Dots Enabling Efficient Ultranarrow Blue Light-Emitting Diodes. *Nano Lett.* **2021,** *21* (17), 7252-7260.
27. Dai, X.; Zhang, Z.; Jin, Y.; Niu, Y.; Cao, H.; Liang, X.; Chen, L.; Wang, J.; Peng, X., Solution-processed, high-performance light-emitting diodes based on quantum dots. *Nature* **2014,** *515* (7525), 96-99.
28. Shen, H.; Cao, W.; Shewmon, N. T.; Yang, C.; Li, L. S.; Xue, J., High-efficiency, low turn-on voltage blue-violet quantum-dot-based light-emitting diodes. *Nano Lett.* **2015,** *15* (2), 1211-1216.
29. Pu, C.; Dai, X.; Shu, Y.; Zhu, M.; Deng, Y.; Jin, Y.; Peng, X., Electrochemically-stable ligands bridge the photoluminescence-electroluminescence gap of quantum dots. *Nat. Commun.* **2020,** *11* (1), 937-946.
30. Qiu, Y.; Gong, Z.; Xu, L.; Huang, Q.; Yang, Z.; Ye, B.; Ye, Y.; Meng, Z.; Zeng, Z.; Shen, Z.; Wu, W.; Zhou, Y.; Hong, Z.; Cheng, Z.; Ye, S.; Hong, H.; Lan, Q.; Li, F.; Guo, T.; Xu, S., Performance Enhancement of Quantum Dot Light-Emitting Diodes via Surface Modification of the Emitting Layer. *ACS Appl. Nano Mater.* **2022,** *5* (2), 2962-2972.
31. Varley, J. B.; Lordi, V., Electrical properties of point defects in CdS and ZnS. *Appl. Phys. Lett.* **2013,** *103* (10), 102103-102106.
32. Wang, Y.-K.; Wan, H.; Xu, J.; Zhong, Y.; Jung, E. D.; Park, S. M.; Teale, S.; Imran, M.; Yu, Y.-J.; Xia, P.; Won, Y.-H.; Kim, K.-H.; Lu, Z.-H.; Liao, L.-S.; Hoogland, S.; Sargent, E. H., Bifunctional Electron-Transporting Agent for Red Colloidal

Quantum Dot Light-Emitting Diodes. *J. Am. Chem. Soc.* **2023,** *145* (11), 6428–6433.

33. Cai, F.; Tu, Y.; Tian, D.; Fang, Y.; Hou, B.; Ishaq, M.; Jiang, X.; Li, M.; Wang, S.; Du, Z., Defect passivation and electron band energy regulation of a ZnO electron transport layer through synergetic bifunctional surface engineering for efficient quantum dot light-emitting diodes. *Nanoscale* **2023,** *15*, 10677-10684.
34. Ding, K.; Chen, H.; Fan, L.; Wang, B.; Huang, Z.; Zhuang, S.; Hu, B.; Wang, L., Polyethylenimine Insulativity-Dominant Charge-Injection Balance for Highly Efficient Inverted Quantum Dot Light-Emitting Diodes. *ACS Appl. Mater. Interfaces* **2017,** *9* (23), 20231-20238.
35. Gao, M.; Tu, Y.; Tian, D.; Yang, H.; Fang, X.; Zhang, F.; Shen, H.; Du, Z., Alleviating Electron Over-Injection for Efficient Cadmium-Free Quantum Dot Light-Emitting Diodes toward Deep-Blue Emission. *ACS Photonics* **2022,** *9* (4), 1400-1408.
36. Murawski, C.; Leo, K.; Gather, M. C., Efficiency Roll-Off in Organic Light-Emitting Diodes. *Adv. Mater.* **2013,** *25* (47), 6801-6827.
37. Lim, J.; Park, Y. S.; Wu, K.; Yun, H. J.; Klimov, V. I., Droop-Free Colloidal Quantum Dot Light-Emitting Diodes. *Nano Lett.* **2018,** *18* (10), 6645-6653.
38. Lee, T.; Kim, B. J.; Lee, H.; Hahm, D.; Bae, W. K.; Lim, J.; Kwak, J., Bright and Stable Quantum Dot Light-Emitting Diodes. *Adv. Mater.* **2022,** *34* (4), 2106276-2106284.
39. Shen, H.; Gao, Q.; Zhang, Y.; Lin, Y.; Lin, Q.; Li, Z.; Chen, L.; Zeng, Z.; Li, X.; Jia, Y.; Wang, S.; Du, Z.; Li, L. S.; Zhang, Z., Visible quantum dot light-emitting diodes with simultaneous high brightness and efficiency. *Nat. Photonics* **2019,** *13* (3), 192-197.
40. Long, R.; Chen, X.; Zhang, X.; Chen, F.; Wu, Z.; Shen, H.; Du, Z., Carboxylic-Free Synthesis of InP Quantum Dots for Highly Efficient and Bright Electroluminescent Device. *Adv. Opt. Mater.* **2023,** *11* (6), 2202594-2202603.
41. Wu, Z.; Liu, P.; Qu, X.; Ma, J.; Liu, W.; Xu, B.; Wang, K.; Sun, X. W., Identifying the Surface Charges and their Impact on Carrier Dynamics in Quantum-Dot Light-Emitting Diodes by Impedance Spectroscopy. *Adv. Opt. Mater.* **2021,** *9* (17), 2100389-2100395.